CLIMATOLOGY

2015 © The Authors, some rights reserved; exclusive licensee American Association for the Advancement of Science. Distributed under a Creative Commons Attribution Non-Commercial License 4.0 (CC BY-NC).
10.1126/sciadv.1400082

Unprecedented 21st century drought risk in the American Southwest and Central Plains

Benjamin I. Cook,[1,2]* Toby R. Ault,[3] Jason E. Smerdon[2]

In the Southwest and Central Plains of Western North America, climate change is expected to increase drought severity in the coming decades. These regions nevertheless experienced extended Medieval-era droughts that were more persistent than any historical event, providing crucial targets in the paleoclimate record for benchmarking the severity of future drought risks. We use an empirical drought reconstruction and three soil moisture metrics from 17 state-of-the-art general circulation models to show that these models project significantly drier conditions in the later half of the 21st century compared to the 20th century and earlier paleoclimatic intervals. This desiccation is consistent across most of the models and moisture balance variables, indicating a coherent and robust drying response to warming despite the diversity of models and metrics analyzed. Notably, future drought risk will likely exceed even the driest centuries of the Medieval Climate Anomaly (1100–1300 CE) in both moderate (RCP 4.5) and high (RCP 8.5) future emissions scenarios, leading to unprecedented drought conditions during the last millennium.

INTRODUCTION

Millennial-length hydroclimate reconstructions over Western North America (*1*–*4*) feature notable periods of extensive and persistent Medieval-era droughts. Such "megadrought" events exceeded the duration of any drought observed during the historical record and had profound impacts on regional societies and ecosystems (*2*, *5*, *6*). These past droughts illustrate the relatively narrow view of hydroclimate variability captured by the observational record, even as recent extreme events (*7*–*9*) highlighted concerns that global warming may be contributing to contemporary droughts (*10*, *11*) and will amplify drought severity in the future (*11*–*15*). A comprehensive understanding of global warming and 21st century drought therefore requires placing projected hydroclimate trends within the context of drought variability over much longer time scales (*16*, *17*). This would also allow us to establish the potential risk (that is, likelihood of occurrence) of future conditions matching or exceeding the severest droughts of the last millennium.

Quantitatively comparing 21st century drought projections from general circulation models (GCMs) to the paleo-record is nevertheless a significant technical challenge. Most GCMs provide soil moisture diagnostics, but their land surface models often vary widely in terms of parameterizations and complexity (for example, soil layering and vegetation). There are few large-scale soil moisture measurements that can be easily compared to modeled soil moisture, and none for intervals longer than the satellite record. Instead, drought is typically monitored in the real world using offline models or indices that can be estimated from more widely measured data, such as temperature and precipitation.

One common metric is the Palmer Drought Severity Index (PDSI) (*18*), widely used for drought monitoring and as a target variable for proxy-based reconstructions (*1*, *2*). PDSI is a locally normalized index of soil moisture availability, calculated from the balance of moisture supply (precipitation) and demand (evapotranspiration). Because PDSI is normalized on the basis of local average moisture conditions, it can be used to compare variability and trends in drought across regions. Average moisture conditions (relative to a defined baseline) are denoted by PDSI = 0; negative PDSI values indicate drier than average conditions (droughts), and positive PDSI values indicate wetter than normal conditions (pluvials). PDSI is easily calculated from GCMs using variables from the atmosphere portion of the model (for example, precipitation, temperature, and humidity) and can be compared directly to observations. However, whereas recent work has demonstrated that PDSI is able to accurately reflect the surface moisture balance in GCMs (*19*), other studies have highlighted concerns that PDSI may overestimate 21st century drying because of its relatively simple soil moisture accounting and lack of direct CO2 effects that are expected to reduce evaporative losses (*12*, *20*, *21*). We circumvent these concerns by using a more physically based version of PDSI (*13*) (based on the Penman-Monteith potential evapotranspiration formulation) in conjunction with soil moisture from the GCMs to demonstrate robust drought responses to climate change in the Central Plains (105°W–92°W, 32°N–46°N) and the Southwest (125°W–105°W, 32°N–41°N) regions of Western North America.

RESULTS

We calculate summer season [June-July-August (JJA)] PDSI and integrated soil moisture from the surface to ~30-cm (SM-30cm) and ~2- to 3-m (SM-2m) depths from 17 GCMs (tables S1 and S2) in phase 5 of the Coupled Model Intercomparison Project (CMIP5) database (*22*). We focus our analyses and presentation on the RCP 8.5 "business-as-usual" high emissions scenario, designed to yield an approximate top-of-atmosphere radiative imbalance of +8.5 W m^{-2} by 2100. We also conduct the same analyses for a more moderate emissions scenario (RCP 4.5).

Over the calibration interval (1931–1990), the PDSI distributions from the models are statistically indistinguishable from the North American Drought Atlas (NADA) (two-sided Kolmogorov-Smirnov test, $p \geq 0.05$), although there are some significant deviations in some models during other historical intervals. North American drought variability during the historical period in both models and observations is driven primarily by ocean-atmosphere teleconnections,

[1]NASA Goddard Institute for Space Studies, 2880 Broadway, New York, NY 10025, USA. [2]Ocean and Climate Physics, Lamont-Doherty Earth Observatory of Columbia University, 61 Route 9W, Palisades, NY 10964, USA. [3]Earth and Atmospheric Sciences, Cornell University, Ithaca, NY 14853, USA.
*Corresponding author. E-mail: benjamin.i.cook@nasa.gov

Downloaded from http://advances.sciencemag.org/ on October 2, 2015

internal variability in the climate system that is likely to not be either consistent across models or congruent in time between the observations and models, and so such disagreements are unsurprising. In the multimodel mean, all three moisture balance metrics show markedly consistent drying during the later half of the 21st century (2050–2099) (Fig. 1; see figs. S1 to S4 for individual models). Drying in the Southwest is more severe (RCP 8.5: PDSI = −2.31, SM-30cm = −2.08, SM-2m = −2.98) than that over the Central Plains (RCP 8.5: PDSI = −1.89, SM-30cm = −1.20, SM-2m = −1.17). In both regions, the consistent cross-model drying trends are driven primarily by the forced response to increased greenhouse gas concentrations (*13*), rather than by any fundamental shift in ocean-atmosphere dynamics [indeed, there is a wide disparity across models regarding the strength and fidelity of the simulated teleconnections over North America (*23*)]. In the Southwest, this forcing manifests as both a reduction in cold season precipitation (*24*) and an increase in potential evapotranspiration (that is, evaporative demand increases in a warmer atmosphere) (*13*, *25*) acting in concert to reduce soil moisture. Even though cold season precipitation is actually expected to increase over parts of California in our Southwest region (*24*, *26*), the increase in evaporative demand is still sufficient to drive a net reduction in soil moisture. Over the Central Plains, precipitation responses during the spring and summer seasons (the main

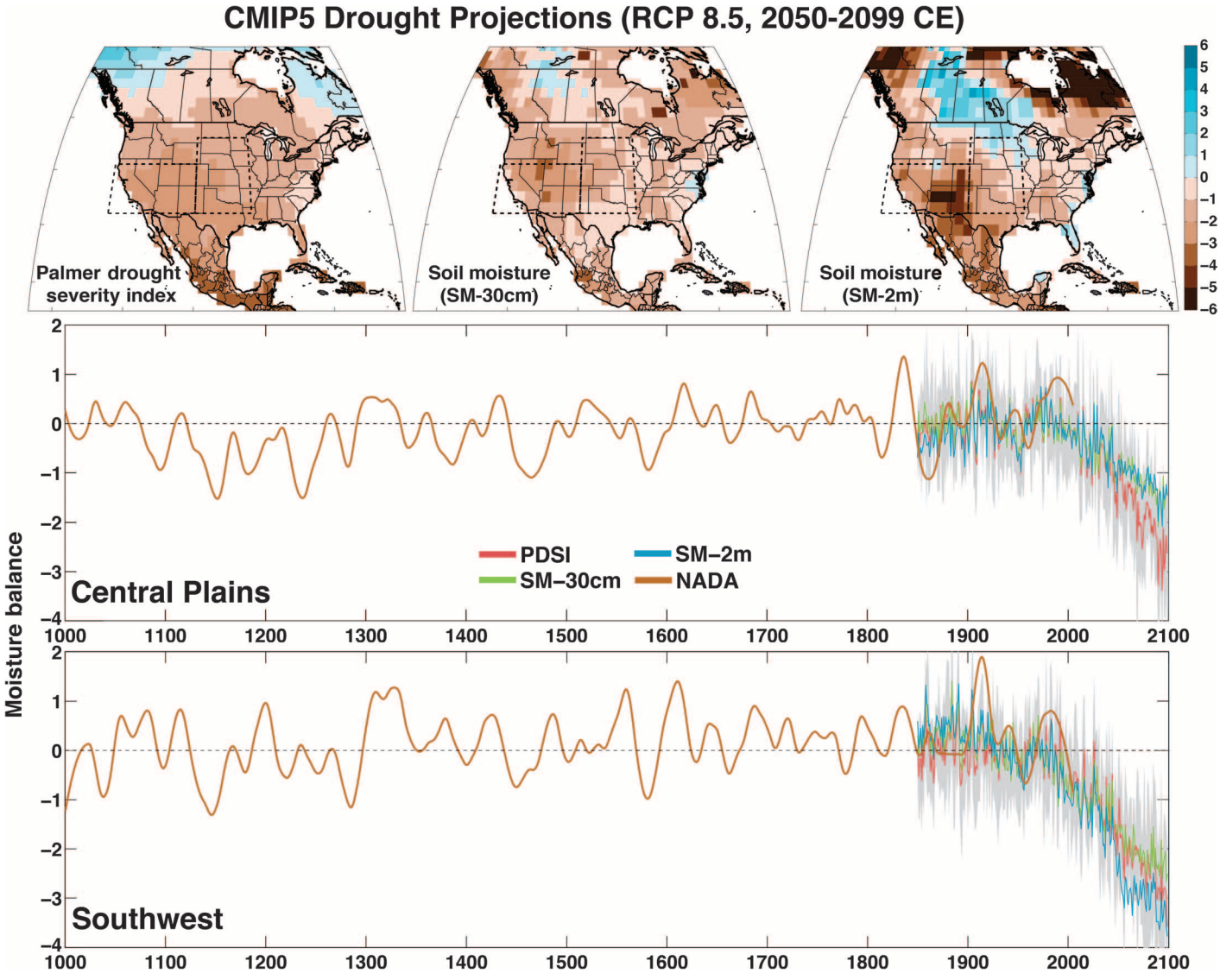

Fig. 1. Top: Multimodel mean summer (JJA) PDSI and standardized soil moisture (SM-30cm and SM-2m) over North America for 2050–2099 from 17 CMIP5 model projections using the RCP 8.5 emissions scenario. SM-30cm and SM-2m are standardized to the same mean and variance as the model PDSI over the calibration interval from the associated historical scenario (1931–1990). Dashed boxes represent the regions of interest: the Central Plains (105°W–92°W, 32°N–46°N) and the Southwest (125°W–105°W, 32°N–41°N). Bottom: Regional average time series of the summer season moisture balance metrics from the NADA and CMIP5 models. The observational NADA PDSI series (brown) is smoothed using a 50-year loess spline to emphasize the low-frequency variability in the paleo-record. Model time series (PDSI, SM-30cm, and SM-2m) are the multimodel means averaged across the 17 CMIP5 models, and the gray shaded area is the multimodel interquartile range for model PDSI.

Downloaded from http://advances.sciencemag.org/ on October 2, 2015

seasons of moisture supply) are less consistent across models, and the drying is driven primarily by the increased evaporative demand. Indeed, this increase in potential evapotranspiration is one of the dominant drivers of global drought trends in the late 21st century, and previous work with the CMIP5 archive demonstrated that the increased evaporative demand is likely to be sufficient to overcome precipitation increases in many regions (*13*). In the more moderate emissions scenario (RCP 4.5), both the Southwest (RCP 4.5: PDSI = −1.49, SM-30cm = −1.63, SM-2m = −2.39) and Central Plains (RCP 4.5: PDSI = −1.21, SM-30cm = −0.89, SM-2m = −1.17) still experience significant, although more modest, drying into the future, as expected (fig. S5).

In both regions, the model-derived PDSI closely tracks the two soil moisture metrics (figs. S6 and S7), correlating significantly for most models and model intervals (figs. S8 and S9). Over the historical simulation, average model correlations (Pearson's r) between PDSI and SM-30cm are +0.86 and +0.85 for the Central Plains and Southwest, respectively. Correlations weaken very slightly for PDSI and SM-2m: +0.84 (Central Plains) and +0.83 (Southwest). The correlations remain strong into the 21st century, even as PDSI and the soil moisture variables occasionally diverge in terms of long-term trends. There is no evidence, however, for systematic differences between the PDSI and modeled soil moisture across the model ensemble. For example, whereas the PDSI trends are drier than the soil moisture condition over the Southwest in the ACCESS1-0 model, PDSI is actually less dry than the soil moisture in the MIROC-ESM and NorESM1-M simulations over the same region (fig. S7). These outlier observations, showing no consistent bias, in conjunction with the fact that the overall comparison between PDSI and modeled soil moisture is markedly consistent, provide mutually consistent support for the characterization of surface moisture balance by these metrics in the model projections.

For estimates of observed drought variability over the last millennium (1000–2005), we use data from the NADA, a tree-ring based reconstruction of JJA PDSI. Comparisons between the NADA and model moisture are shown in the bottom panels of Fig. 1. In the NADA, both the Central Plains (Fig. 2) and Southwest (Fig. 3) are drier during the Medieval megadrought interval (1100–1300 CE) than either the Little

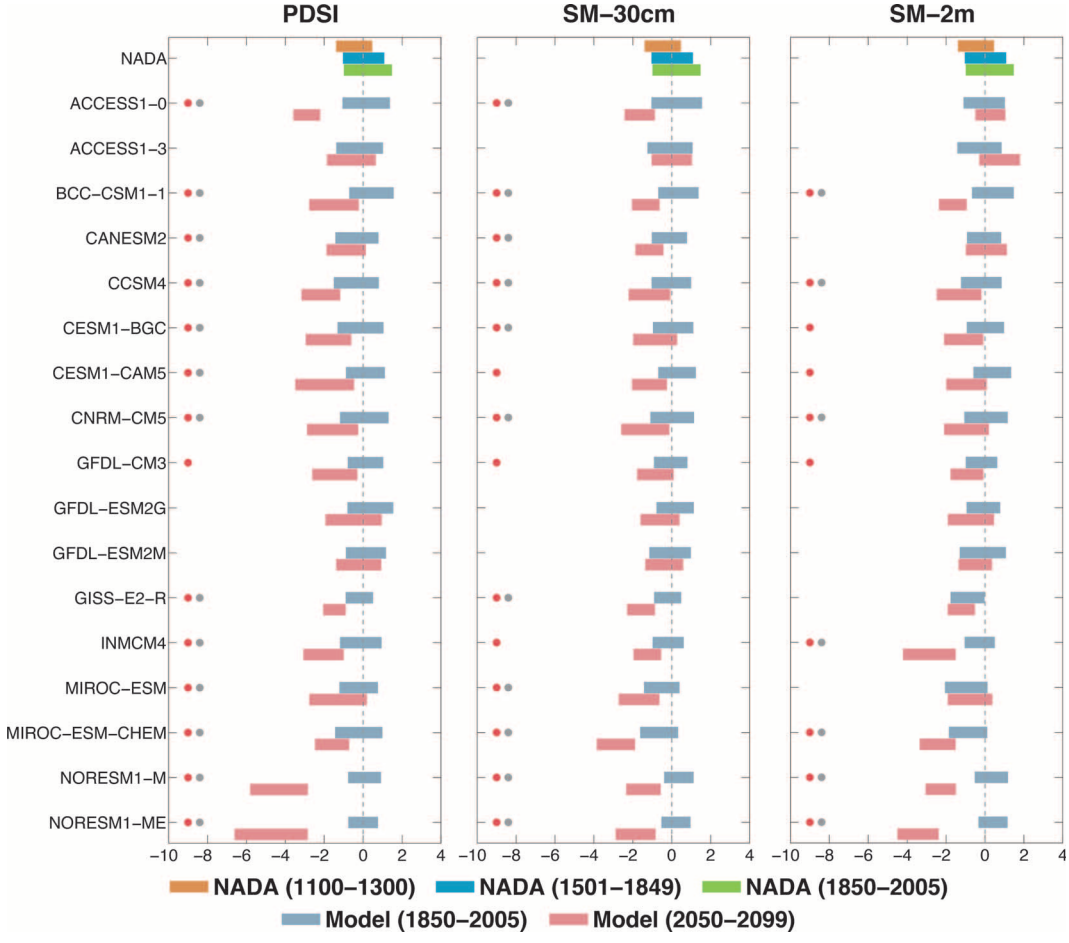

Fig. 2. Interquartile range of PDSI and soil moisture from the NADA and CMIP5 GCMs, calculated over various time intervals for the Central Plains. The groups of three stacked bars at the top of each column are from the NADA PDSI: 1100–1300 (the time of the Medieval-era megadroughts, brown), 1501–1849 (the Little Ice Age, blue), and 1850–2005 (the historical period, green). Purple and red bars are for the modeled historical period (1850–2005) and late 21st century (2050–2099) period, respectively. Red dots indicate model 21st century drought projections that are significantly drier than the model simulated historical periods. Gray dots indicate model 21st century drought projections that are significantly drier than the Medieval-era megadrought period in the NADA.

Downloaded from http://advances.sciencemag.org/ on October 2, 2015

Ice Age (1501–1849) or historical periods (1850–2005). For nearly all models, the 21st century projections under the RCP 8.5 scenario reveal dramatic shifts toward drier conditions. Most models (indicated with a red dot) are significantly drier (one-sided Kolmogorov-Smirnov test, $p \leq 0.05$) in the latter part of the 21st century (2050–2099) than during their modeled historical intervals (1850–2005). Strikingly, shifts in projected drying are similarly significant in most models when measured against the driest and most extreme megadrought period of the NADA from 1100 to 1300 CE (gray dots). Results are similar for the more moderate RCP 4.5 emissions scenario (figs. S10 and S11), which still indicates widespread drying, albeit at a reduced magnitude for many models. Although there is some spread across the models and metrics, only two models project wetter conditions in RCP 8.5. In the Central Plains, SM-2m is wetter in ACCESS1-3, with little change in SM-30cm and slightly wetter conditions in PDSI. In the Southwest, CanESM2 projects markedly wetter SM-2m conditions; PDSI in the same model is slightly wetter, whereas SM-30cm is significantly drier.

When the RCP 8.5 multimodel ensemble is pooled together (Fig. 4), projected changes in the Central Plains and Southwest (2050–2099 CE) for all three moisture balance metrics are significantly drier compared to both the modern model interval (1850–2005 CE) and 1100–1300 CE in the NADA (one-sided Kolmogorov-Smirnov test, $p \leq 0.05$). In the case of SM-2m in the Southwest, the density function is somewhat flattened, with an elongated right (wet) tail. This distortion arises from the disproportionate contribution to the density function from the wetting in the five CanESM2 ensemble members. Even with this contribution, however, the SM-2m drying in the multimodel ensemble is still significant. Results are nearly identical for the pooled RCP 4.5 multimodel ensemble (fig. S12), which still indicates a significantly drier late 21st century compared to either the historical interval or Medieval megadrought period.

With this shift in the full hydroclimate distribution, the risk of decadal or multidecadal drought occurrences increases substantially. We calculated the risk (*17*) of decadal or multidecadal drought occurrences for two periods in our multimodel ensemble: 1950–2000 and 2050–2099 (Fig. 5). During the historical period, the risk of a multidecadal megadrought is quite small: <12% for both regions and all moisture metrics. Under RCP 8.5, however, there is ≥80% chance of a multidecadal drought during 2050–2099 for PDSI and SM-30cm in the Central Plains and for all three moisture metrics in the Southwest. Drought risk is reduced slightly in RCP 4.5 (fig. S13), with largest reductions in multidecadal drought risk over the Central Plains. Ultimately, the consistency of our results suggests an exceptionally high risk of a multidecadal megadrought occurring over the Central Plains and Southwest regions during the late 21st century, a level of aridity exceeding even the persistent megadroughts that characterized the Medieval era.

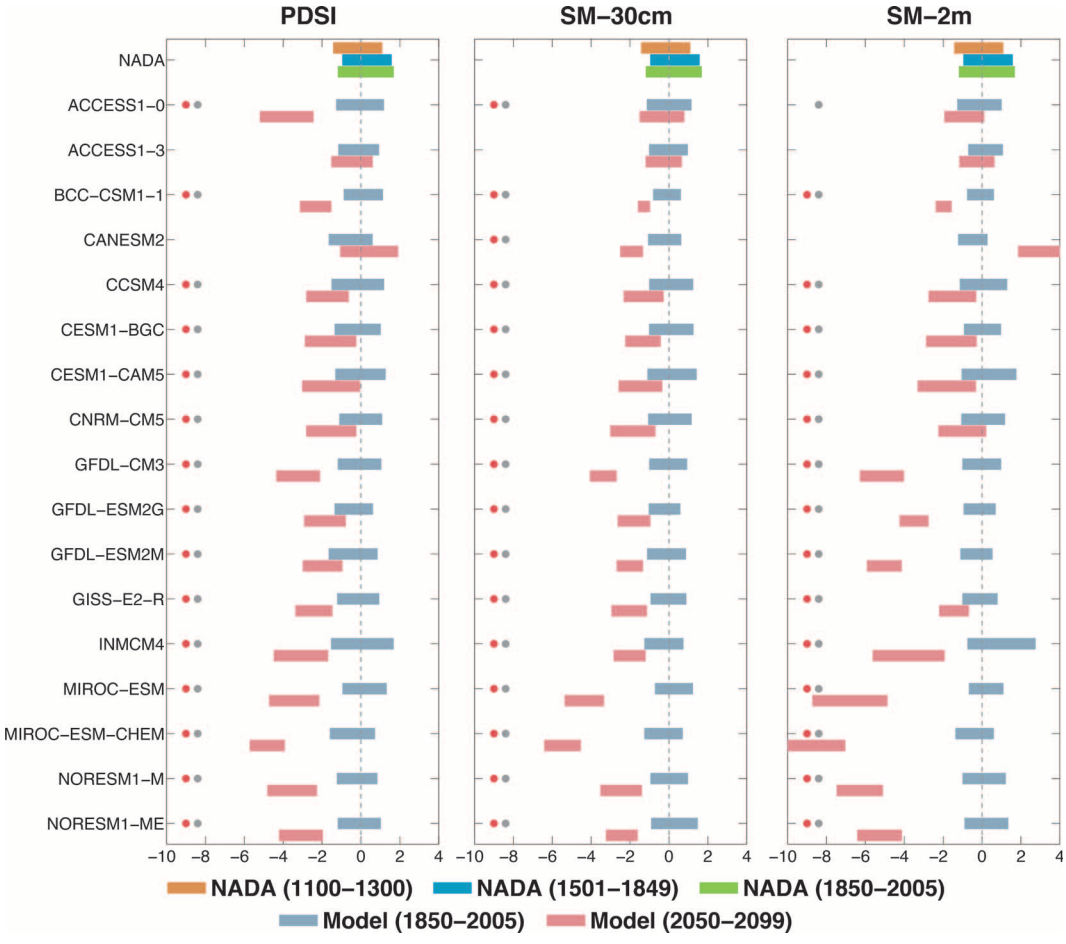

Fig. 3. Same as Fig. 2, but for the Southwest.

Downloaded from http://advances.sciencemag.org/ on October 2, 2015

DISCUSSION

Within the body of literature investigating North American hydroclimate, analyses of drought variability in the historical and paleoclimate records are often separate from discussions of global warming–induced changes in future hydroclimate. This disconnection has traditionally made it difficult to place future drought projections within the context of observed and reconstructed natural hydroclimate variability. Here,

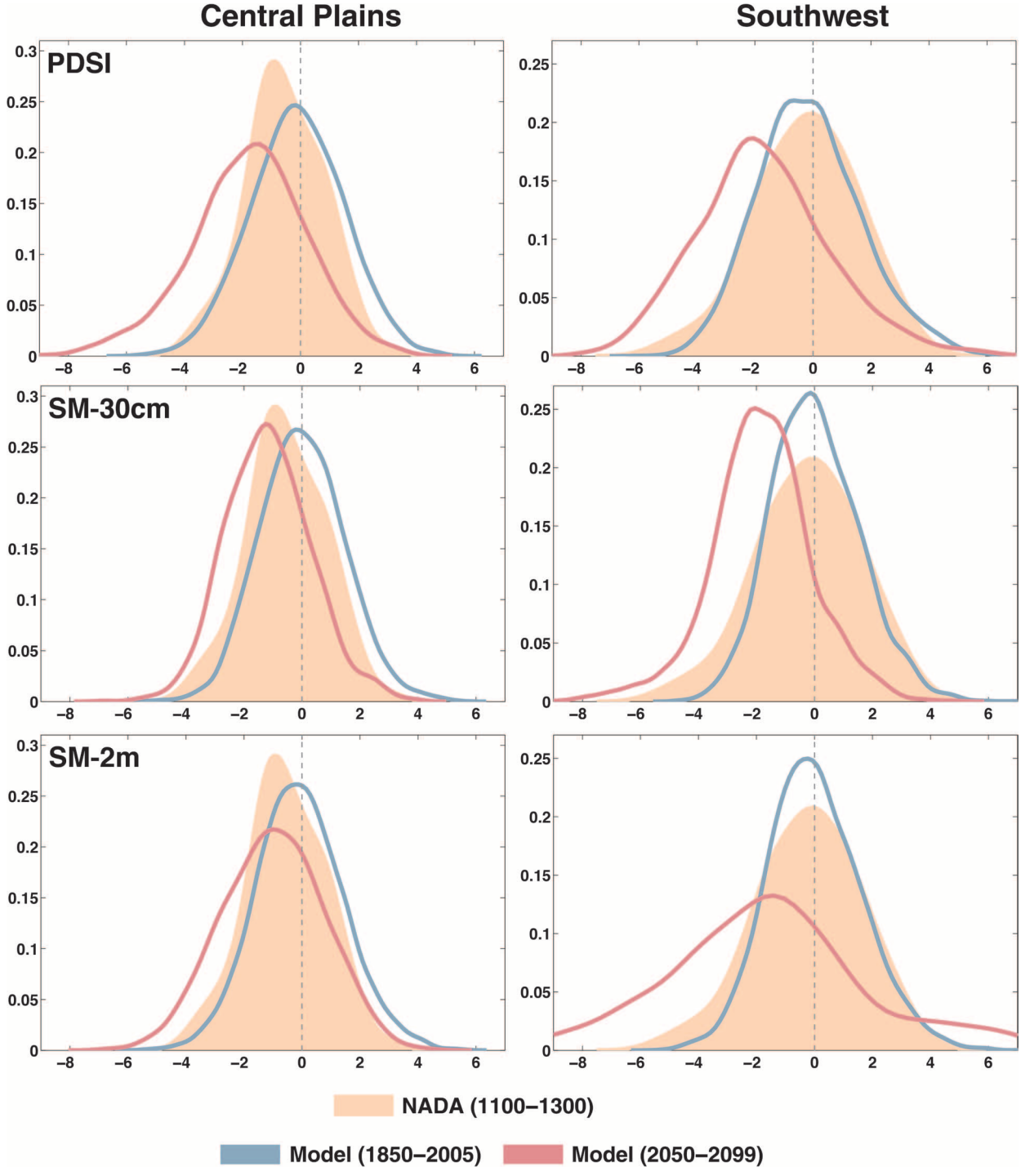

Fig. 4. Kernel density functions of PDSI, SM-30cm, and SM-2m for the Central Plains and Southwest, calculated from the NADA and the GCMs. The NADA distribution (brown shading) is from 1100–1300 CE, the timing of the medieval megadroughts. Blue lines represent model distributions calculated from all years from all models pooled over the historical scenario (1850–2005 CE). Red lines are for all model years pooled from the RCP 8.5 scenario (2050–2099 CE).

Downloaded from http://advances.sciencemag.org/ on October 2, 2015

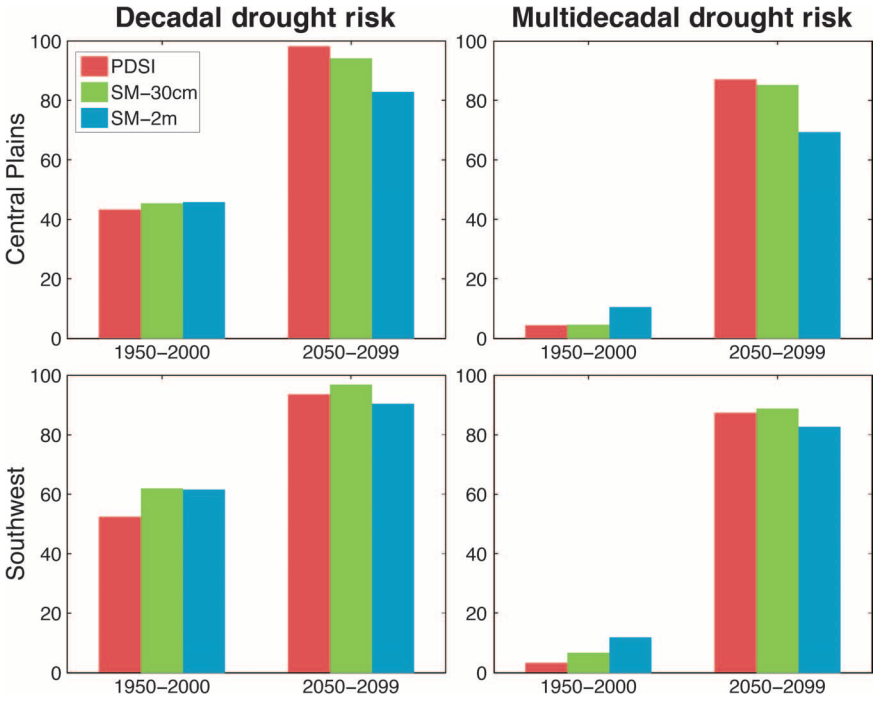

Fig. 5. Risk (percent chance of occurrence) of decadal (11-year) and multidecadal (35-year) drought, calculated from the multimodel ensemble for PDSI, SM-30cm, and SM-2m. Risk calculations are conducted for two separate model intervals: 1950–2000 (historical scenario) and 2050–2099 (RCP 8.5). Results for the Central Plains are in the top row, and those for the Southwest are in the bottom row.

we have demonstrated that the mean state of drought in the late 21st century over the Central Plains and Southwest will likely exceed even the most severe megadrought periods of the Medieval era in both high and moderate future emissions scenarios, representing an unprecedented fundamental climate shift with respect to the last millennium. Notably, the drying in our assessment is robust across models and moisture balance metrics. Our analysis thus contrasts sharply with the recent emphasis on uncertainty about drought projections for these regions (*21*, *27*), including the most recent Intergovernmental Panel on Climate Change assessment report (*28*).

Our results point to a remarkably drier future that falls far outside the contemporary experience of natural and human systems in Western North America, conditions that may present a substantial challenge to adaptation. Human populations in this region, and their associated water resources demands, have been increasing rapidly in recent decades, and these trends are expected to continue for years to come (*29*). Future droughts will occur in a significantly warmer world with higher temperatures than recent historical events, conditions that are likely to be a major added stress on both natural ecosystems (*30*) and agriculture (*31*). And, perhaps most importantly for adaptation, recent years have witnessed the widespread depletion of nonrenewable groundwater reservoirs (*32*, *33*), resources that have allowed people to mitigate the impacts of naturally occurring droughts. In some cases, these losses have even exceeded the capacity of Lake Mead and Lake Powell, the two major surface reservoirs in the region (*34*, *35*). Combined with the likelihood of a much drier future and increased demand, the loss of groundwater and higher temperatures will likely exacerbate the impacts of future droughts, presenting a major adaptation challenge for managing ecological and anthropogenic water needs in the region.

MATERIALS AND METHODS

Estimates of drought variability over the historical period and the last millennium used the latest version of the NADA (*1*), a tree ring–based reconstruction of summer season (JJA) PDSI. All statistics were based on regional PDSI averages over the Central Plains (105°W–92°W, 32°N–46°N) and the Southwest (125°W–105°W, 32°N–41°N). We restricted our analysis to 1000–2005 CE; before 1000 CE, the quality of the reconstruction in these regions declines.

The 21st century drought projections used output from GCM simulations in the CMIP5 database (*22*) (table S1). All models represent one or more continuous ensemble members from the historical (1850–2005 CE) and RCP 4.5 (15 models available) and 8.5 (17 models available) emissions scenarios (2006–2099 CE). We used the same methodology as in (*13*) to calculate model PDSI for the full interval (1850–2099 CE), using the Penman-Monteith formulation of potential evapotranspiration. The baseline period for calibrating and standardizing the model PDSI anomalies was 1931–1990 CE, the same baseline period as the NADA PDSI. Negative model PDSI values therefore indicate drier conditions than the average for 1931–1990.

To augment the model PDSI calculations and comparisons with observed drought variability in the NADA, we also calculated standardized soil moisture metrics from the GCMs for two depths: ~30 cm (SM-30cm) and ~2 to 3 m (SM-2m) (table S2). For these soil moisture metrics, the total soil moisture from the surface was integrated to these depths and averaged over JJA. At each grid cell, we then standardized SM-30cm and SM-2m to match the same mean and interannual SD for the model PDSI over 1931–1990. This allows for direct comparison of variability and trends between model PDSI and model soil moisture and between the model metrics (PDSI, SM-30cm, and SM-2m) and the NADA (PDSI) while still independently preserving any low-frequency variability or trends in the soil moisture that may be distinct from the PDSI calculation. The soil moisture standardization does not impose any artificial constraints that would force the three metrics to agree in terms of variability or future trends, allowing SM-30cm and SM-2m to be used as indicators of drought largely independent of PDSI.

Risk of decadal and multidecadal megadrought occurrence in the multimodel ensemble is estimated from 1000 Monte Carlo realizations of each moisture balance metric (PDSI, SM-30cm, and SM-2m), as in (*17*). This method entails estimating the mean and SD of a given drought index (for example, PDSI or soil moisture) over a reference period (1901–2000), then subtracting that mean and SD from the full record (1850–2100) to produce a modified z score. The differences between the reference mean and SD are then used to conduct (white noise) Monte Carlo simulations of the future (2050–2100) to emulate the statistics of that era. The fraction of Monte Carlo realizations exhibiting a decadal or multidecadal drought are then calculated from each Monte Carlo simulation of each experiment in both regions considered here. Finally, these risks from each model are averaged together to yield the overall risk estimates reported here. Additional details on the methodology can be found in (*17*).

Downloaded from http://advances.sciencemag.org/ on October 2, 2015

SUPPLEMENTARY MATERIALS

Supplementary material for this article is available at http://advances.sciencemag.org

Fig. S1. For the individual models, ensemble mean soil moisture balance (PDSI, SM-30cm, and SM-2m) for 2050–2099: ACCESS1.0, ACCESS1.3, BCC-CSM1.1, and CanESM2.

Fig. S2. Same as fig. S1, but for CCSM4, CESM1-BGC, CESM-CAM5, and CNRM-CM5.

Fig. S3. Same as fig. S1, but for GFDL-CM3, GFDL-ESM2G, GFDL-ESM2M, and GISS-E2-R.

Fig. S4. Same as fig. S1, but for INMCM4.0,MIROC-ESM, MIROC-ESM-CHEM, NorESM1-M, and NorESM1-ME models.

Fig. S5. Same as Fig. 1, but for the RCP 4.5 scenario.

Fig. S6. Regional average moisture balance time series (historical + RCP 8.5) from the first ensemble member of each model over the Central Plains.

Fig. S7. Same as fig. S6, but for the Southwest.

Fig. S8. Pearson's correlation coefficients for three time intervals from the models over the Central Plains: PDSI versus SM-30cm, PDSI versus SM-2m, and SM-30cm versus SM-2m.

Fig. S9. Same as fig. S8, but for the Southwest.

Fig. S10. Same as Fig. 2, but for the RCP 4.5 scenario.

Fig. S11. Same as Fig. 3, but for the RCP 4.5 scenario.

Fig. S12. Same as Fig.4, but for the RCP 4.5 scenario.

Fig. S13. Same as Fig. 5, but for the RCP 4.5 scenario.

Table S1. Continuous model ensembles from the CMIP5 experiments (1850–2099, historical + RCP8.5 scenario) used in this analysis, including the modeling center or group that supplied the output, the number of ensemble members, and the approximate spatial resolution.

Table S2. The number of soil layers integrated for our CMIP5 soil moisture metrics (SM-30cm and SM-2m), and the approximate depth of the bottom soil layer.

REFERENCES AND NOTES

1. E. R. Cook, R. Seager, M. A. Cane, D. W. Stahle, North American drought: Reconstructions, causes, and consequences. *Earth Sci. Rev.* **81**, 93–134 (2007).
2. E. R. Cook, R. Seager, R. R. Heim Jr., R. S. Vose, C. Herweijer, C. Woodhouse, Megadroughts in North America: Placing IPCC projections of hydroclimatic change in a long-term palaeoclimate context. *J. Quat. Sci.* **25**, 48–61 (2010).
3. D. M. Meko, C. A. Woodhouse, C. A. Baisan, T. Knight, J. J. Lukas, M. K. Hughes, M. W. Salzer, Medieval drought in the upper Colorado River Basin. *Geophys. Res. Lett.* **34**, 10705 (2007).
4. C. A. Woxodhouse, D. M. Meko, G. M. MacDonald, D. W. Stahle, E. R. Cook, A 1,200-year perspective of 21st century drought in Southwester North America. *Proc. Natl. Acad. Sci. U.S.A.* **107**, 21283–21288 (2010).
5. S. Stine, Extreme and persistent drought in California and Patagonia during mediaeval time. *Nature* **369**, 546–549 (1994).
6. C. A. Woodhouse, J. T. Overpeck, 2000 years of drought variability in the Central United States. *Bull. Am. Meteorol. Soc.* **79**, 2693–2714 (1998).
7. M. Hoerling, J. Eischeid, A. Kumar, R. Leung, A. Mariotti, K. Mo, S. Schubert, R. Seager, Causes and predictability of the 2012 Great Plains drought. *Bull. Am. Meteorol. Soc.* **95**, 269–282 (2014).
8. R. Seager, L. Goddard, J. Nakamura, N. Henderson, D. E. Lee, Dynamical causes of the 2010/11 Texas–Northern Mexico drought. *J. Hydrometeor.* **15**, 39–68 (2014).
9. H. Wang, S. Schubert, R. Koster, Y.-G. Ham, M. Suarez, On the role of SST forcing in the 2011 and 2012 extreme U.S. heat and drought: A study in contrasts. *J. Hydrometeor.* **15**, 1255–1273 (2014).
10. D. Griffin, K. J. Anchukaitis, How unusual is the 2012–2014 California drought? *Geophys. Res. Lett.* **41**, 2014GL062433 (2014).
11. R. Seager, M. Hoerling, Atmosphere and ocean origins of North American droughts. *J. Clim.* **27**, 4581–4606 (2014).
12. E. J. Burke, Understanding the sensitivity of different drought metrics to the drivers of drought under increased atmospheric CO_2. *J. Hydrometeor.* **12**, 1378–1394 (2011).
13. B. I. Cook, J. E. Smerdon, R. Seager, S. Coats, Global warming and 21st century drying. *Clim. Dyn.* **43**, 2607–2627 (2014).
14. A. Dai, Drought under global warming: A review. *WIREs Clim. Change* **2**, 45–65 (2011).
15. A. Dai, Increasing drought under global warming in observations and models. *Nat. Clim. Change* **3**, 52–58 (2013).
16. T. R. Ault, J. E. Cole, J. T. Overpeck, G. T. Pederson, S. St. George, B. Otto-Bliesner, C. A. Woodhouse, C. Deser, The continuum of hydroclimate variability in Western North America during the last millennium. *J. Clim.* **26**, 5863–5878 (2013).
17. T. R. Ault, J. E. Cole, J. T. Overpeck, G. T. Pederson, D. M. Meko, Assessing the risk of persistent drought using climate model simulations and paleoclimate data. *J. Clim.* **27**, 7529–7549 (2014).
18. W. C. Palmer, Meteorological Drought (U.S. Weather Bureau, Washington, DC, 1965).
19. J. E. Smerdon, B. I. Cook, E. R. Cook, R. Seager, J. Clim., in press.
20. E. J. Burke, S. J. Brown, Evaluating uncertainties in the projection of future drought. *J. Hydrometeor.* **9**, 292–299 (2008).
21. M. P. Hoerling, J. K. Eischeid, X.-W. Quan, H. F. Diaz, R. S. Webb, R. M. Dole, D. R. Easterling, Is a transition to semipermanent drought conditions imminent in the U.S. Great Plains? *J. Clim.* **25**, 8380–8386 (2012).
22. K. E. Taylor, R. J. Stouffer, G. A. Meehl, An overview of CMIP5 and the experiment design. *Bull. Am. Meteorol. Soc.* **93**, 485–498 (2012).
23. S. Coats, J. E. Smerdon, B. I. Cook, R. Seager, Stationarity of the tropical pacific teleconnection to North America in CMIP5/PMIP3 model simulations. *Geophys. Res. Lett.* **40**, 4927–4932 (2013).
24. R. Seager, D. Neelin, I. Simpson, H. Liu, N. Henderson, T. Shaw, Y. Kushnir, M. Ting, B. Cook, Dynamical and thermodynamical causes of large-scale changes in the hydrological cycle over North America in response to global warming. *J. Clim.* **27**, 7921–7948 (2014).
25. J. Scheff, D. M. W. Frierson, Scaling potential evapotranspiration with greenhouse warming. *J. Clim.* **27**, 1539–1558 (2013).
26. J. D. Neelin, B. Langenbrunner, J. E. Meyerson, A. Hall, N. Berg, California winter precipitation change under global warming in the Coupled Model Intercomparison Project phase 5 ensemble. *J. Clim.* **26**, 6238–6256 (2013).
27. J. Sheffield, E. F. Wood, M. L. Roderick, Little change in global drought over the past 60 years. *Nature* **491**, 435–438 (2012).
28. B. Kirtman, S. B. Power, G. J. Adedoyin, R. Boer, I. Bojariu, F. J. Camilloni, A. M. Doblas-Reyes, A. M. Fiore, M. Kimoto, G. A. Meehl, M. Prather, A. Sarr, C. Schar, R. Sutton, G. J. van Oldenborgh, G. Vecchi, H. J. Wang, Climate Change 2013: The Physical Science Basis. Contribution of Working Group I to the Fifth Assessment Report of the Intergovernmental Panel on Climate Change (Cambridge University Press, Cambridge, UK, and New York, NY, USA, 2013), chap. Near-term Climate Change: Projections and Predictability.
29. G. M. MacDonald, Water, climate change, and sustainability in the southwest. *Proc. Natl. Acad. Sci. U.S.A.* **107**, 21256–21262 (2010).
30. A. P. Williams, C. D. Allen, A. K. Macalady, D. Griffin, C. A. Woodhouse, D. M. Meko, T. W. Swetnam, S. A. Rauscher, R. Seager, H. D. Grissino-Mayer, J. S. Dean, Ed. R. Cook, C. Gangodagamage, M. Cai, N. G. McDowell, Temperature as a potent driver of regional forest drought stress and tree mortality. *Nat. Clim. Change* **3**, 292–297 (2013).
31. D. B. Lobell, M. J. Roberts, W. Schlenker, N. Braun, B.B. Little, R. M. Rejesus, G. L. Hammer, Greater sensitivity to drought accompanies maize yield increase in the U.S. midwest. *Science* **344**, 516–519 (2014).
32. D. Long, B. R. Scanlon, L. Longuevergne, A. Y. Sun, D. N. Fernando, H. Save, GRACE satellite monitoring of large depletion in water storage in response to the 2011 drought in Texas. *Geophys. Res. Lett.* **40**, 3395–3401 (2013).
33. B. R. Scanlon, C. C. Faunt, L. Longuevergne, R. C. Reedy, W. M. Alley, V. L. Mcguire, P. B. McMahon, Groundwater depletion and sustainability of irrigation in the US high plains and Central Valley. *Proc. Natl. Acad. Sci. U.S.A.* **109**, 9320–9325 (2012).
34. S. L. Castle, B. F. Thomas, J. T. Reager, M. Rodell, S. C. Swenson, J. S. Famiglietti, Groundwater depletion during drought threatens future water security of the Colorado River Basin. *Geophys. Res. Lett.* **41**, 5904–5911 (2014).
35. J. S. Famiglietti, M. Lo, S. L. Ho, J. Bethune, K. J. Anderson, T. H. Syed, S. C. Swenson, C. R. de Linage, M. Rodell, Satellites measure recent rates of groundwater depletion in California's Central Valley. *Geophys. Res. Lett.* **38**, L03403 (2011).

Acknowledgments: We thank H. Liu and N. Henderson for invaluable computing support at Lamont-Doherty Earth Observatory and E. Cook for providing the NADA data. All model data are freely available on the CMIP5 archive. Finally, we thank two anonymous reviewers who provided comments that greatly improved the manuscript. Lamont contribution #7865. **Funding:** Funding for B.I.C. for this work was provided by the NASA Modeling, Analysis, and Prediction Program and NASA Strategic Science. Support for J.E.S. came from NSF Awards AGS-1243204 ("Collaborative Research: EaSM2–Linking Near Term Future Changes in Weather and Hydroclimate in Western North America to Adaptation for Ecosystem and Water Management") and AGS-1401400 ("P2C2: Continental Scale Droughts in North America: Their Frequency, Character and Causes Over the Past Millenium and Near Term Future"), and NOAA Award NAOR4310137 ("Global Decadal Hydroclimate Variability, Predictability and Change: A Data-Enriched Modeling Study"). Funding for T.R.A. was provided by startup funds from Cornell University's College of Agriculture and Life Sciences (CALS). **Author contributions:** B.I.C., T.R.A., and J.E.S. conceived of the study. B.I.C. conducted all the analyses except the risk calculations and wrote the paper. T.R.A. conducted the risk calculations. T.R.A. and J.E.S. contributed feedback to the analyses and writing.

Submitted 17 November 2014
Accepted 15 January 2015
Published 12 February 2015
10.1126/sciadv.1400082

Citation: B. I. Cook, T. R. Ault, J. E. Smerdon, Unprecedented 21st century drought risk in the American Southwest and Central Plains. *Sci. Adv.* **1**, e1400082 (2015).

Downloaded from http://advances.sciencemag.org/ on October 2, 2015

ScienceAdvances
AAAS

Unprecedented 21st century drought risk in the American Southwest and Central Plains

Benjamin I. Cook, Toby R. Ault and Jason E. Smerdon (February 12, 2015)

Sci Adv 2015, 1:.
doi: 10.1126/sciadv.1400082

This article is publisher under a Creative Commons license. The specific license under which this article is published is noted on the first page.

For articles published under CC BY licenses, you may freely distribute, adapt, or reuse the article, including for commercial purposes, provided you give proper attribution.

For articles published under CC BY-NC licenses, you may distribute, adapt, or reuse the article for non-commerical purposes. Commercial use requires prior permission from the American Association for the Advancement of Science (AAAS). You may request permission by clicking here.

The following resources related to this article are available online at http://advances.sciencemag.org. (This information is current as of October 2, 2015):

Updated information and services, including high-resolution figures, can be found in the online version of this article at:
http://advances.sciencemag.org/content/1/1/e1400082.full.html

Supporting Online Material can be found at:
http://advances.sciencemag.org/content/suppl/2015/02/11/1.1.e1400082.DC1.html

This article **cites 32 articles,**4 of which you can be accessed free:
http://advances.sciencemag.org/content/1/1/e1400082#BIBL

Downloaded from http://advances.sciencemag.org/ on October 2, 2015

Science Advances (ISSN 2375-2548) publishes new articles weekly. The journal is published by the American Association for the Advancement of Science (AAAS), 1200 New York Avenue NW, Washington, DC 20005. Copyright is held by the Authors unless stated otherwise. AAAS is the exclusive licensee. The title Science Advances is a registered trademark of AAAS